

A Novel Technique for Asymmetrical Fault Detection in DFIG based Wind-Farm

R.K. Dubey

Department of Electrical & Electronics Engineering, Manipal Institute of Technology, Udipi-576104
e-mail:rahul.dubey2011@gmail.com,

Abstract

This paper proposes a novel technique for asymmetrical fault detection (LLL-G) in DFIG based wind farm using wavelet based energy function. In this study, there are six wind turbine driven DFIG are grouping together to make wind farm and 9 MW power is feeding to the grid. Further, the rotor is supplied by a bidirectional PWM converter for the control of active and reactive power flows from DFIG to the grid. In the case study, the three-phase fault is created in the grid and proposed algorithm detects the fault with in one and half cycles for 60 Hz system. A new diagnostic method based on the grid modulating signals pre-processing by Discrete Wavelet Transform (DWT) is here proposed to detect grid faults dynamically over time. Simulation results demonstrate the effectiveness of the proposed approach under time-varying conditions

Keywords: Doubly Fed Induction Generator (DFIG), Asymmetrical fault (LLL-G), Wavelet transform, Wavelet Energy.

1. Introduction

Research in the area of fault diagnosis and condition monitoring of wind generators has become a keen interest as the renewable energy became a viable solution for future energy demand and environmental pollution [1]-[4]. Wind generators used for high-power range (660 kW to 2 MW) are mainly wound-rotor synchronous generators and doubly-fed induction generators (DFIGs) [5]. Normally, 690-V DFIGs are used in this power range and relate to major market share. The accurate condition-monitoring and fault-detection method is necessary to reduce the operating and maintenance costs of wind energy based systems. In particular, with plan of offshore installations, which makes it more inaccessible, it is vital to simultaneously increase reliability and service interval.

Like every electrical machine, wind generators are prone to electromechanical faults and require attention at the incipient stage to avoid escalation of the fault to cause a breakdown or major damage. Faults may occur in stator, rotor, bearings, air gap (eccentricity), etc. However, a literature survey shows that bearing faults and stator insulation breakdown cause the majority of machine failures [6]. Induction-machine stator winding insulation degradation is one of the major (about 40%) causes of machine failure [7]. Stator faults begin with degradation of the insulation between turns, and consequently, an interturn short circuit occurs.

Fault-diagnostic methods for squirrel-cage induction motors have been extensively studied in the available literature, and commercial systems for diagnosis of mechanical problems such as broken rotor bars using motor-current signature analysis (MCSA) and bearing faults using vibration analysis are also proposed [8]. However, fault diagnosis for DFIGs has remained little explored. Some research has already been done on stator interturn-fault diagnosis of DFIGs in the last five years, and a literature survey was made to explore existing methods. It suggests that existing techniques are based on vibration analysis or MCSA of stator current [10]. However, these methods have shortcomings due to the need of sophisticated vibration-sensing equipment that is partly invasive, requiring physical installation of sensors on the generator [4] or based on experimental results alone, without complete theoretical basis and fails to prove reliable detections when the DFIG operates under imbalanced-load conditions.

The control schemes used in DFIGs are typically of five types [11], but the most popular schemes are based on a DFIG with static Kramer drive and a DFIG with back-to-back converter as shown in Figure 1[6]. DFIGs used as wind generators are grid connected and are frequently subjected to imbalanced load in three phases. Hence, it is essential to justify the existence of frequency used for fault detection with suitable theory and analysis in order to discover an unambiguous fault-detection technique in the presence of imbalanced load in DFIGs. The objective of this paper is to therefore develop a fault-diagnostic method that could be applied to any DFIG, irrespective of its control scheme, and provide unambiguous fault detection in spite of imbalanced loading. A new diagnostic method based on the grid modulating signals pre-processing by Discrete Wavelet Transform (DWT) is here proposed to detect grid faults dynamically over time. Simulation results demonstrate the effectiveness of the proposed approach under time-varying conditions.

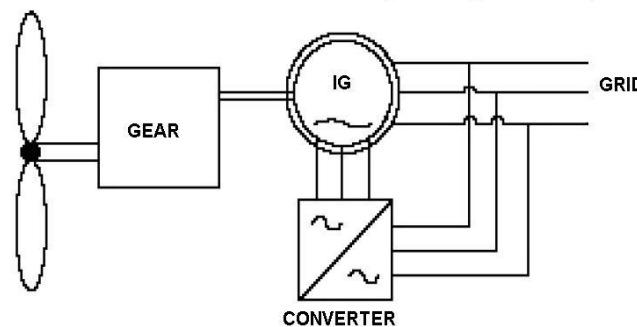


Figure 1. Principle of DFIG connected to a wind turbine

This paper is organized as follows. In Section II, asymmetrical fault (LLL-G) detection methodology is analyzed. Section III describes modeling of the DFIG with asymmetrical fault (LLL-G) and the simulation results. The proposed wavelet energy functions for fault detection in presence of DFIG wind farm are described in Section IV. Section V reveals the general conclusions followed by the references.

2. Detection Methodology

Wavelet Theory is the mathematics, which deals with non-stationary signals, using a set of components that look like small waves, called wavelets. It provides multiple resolutions in both time and frequency. It is a linear transformation like the Fourier transform with one important difference. It allows time localization of a given signal with different frequency components.

➤ Continuous Wavelet Transform

Continuous Wavelet Transform (CWT) of a signal $x(t)$ is defined as

$$CWT(a,b) = \int_{-\infty}^{\infty} x(t) * \frac{1}{\sqrt{a}} * \Psi^* \left(\frac{t-b}{a} \right) dt \quad (1)$$

Where $\psi(t)$ is the base function or mother wavelet, "*" denotes a complex conjugate and $a, b \in \mathbb{R}$, are the translation parameters, respectively. \mathbb{R} is the real number system. [16]

2.1 Discrete Wavelet Transform

The base functions are generated discretely to avoid redundant information by selecting $a = a_0^m$ and $b = nb_0 a_0^m$ [5]. Thus, discrete wavelet transform (DWT) is defined as

$$DWT(m,n) = 2^{-\frac{m}{2}} \sum_m \sum_n x(n) \Psi^* \left(\frac{t-n2^m}{2^m} \right) \quad (2)$$

Where, the discretized mother wavelet is

$$\Psi_{m,n}(t) = \frac{1}{\sqrt{a_0^m}} \Psi \left(\frac{t-nb_0a_0^m}{a_0^m} \right) \quad (3)$$

a_0, b_0 are fixed constant with $a_0 > 1, b_0 > 1$, $n \in \mathbb{Z}$ where \mathbb{Z} is set of integers.

In discrete case, to analyze the signal at different scales filters of different cut-off frequencies are used. Signal is passed through a series of high-pass filter (HPF) and low-pass filter (LPF) to analyze the high frequency and low frequency components respectively.

2.2 Multiresolution Analysis (MRA)

MRA allows the signal to decompose into various levels of resolution. Course resolution level contains approximate Information about low frequency components and retains the main features of original signal. Detailed information about the high frequency components are retained from the level with finer resolution [16] this is an effective method in which a signal is decomposed into scales with different frequency and time resolutions and can be implemented by using only two filters, one HPF and another LPF. Then the results are down sampled by a factor of two and same two filters are applied to the output of LPF from the previous stage. From the mother wavelet, the HPF derived and measure the details in a particular input. On the other hand, the LPF delivers a smooth version of the input signal and this filter is derived from the mother wavelet scaling function.

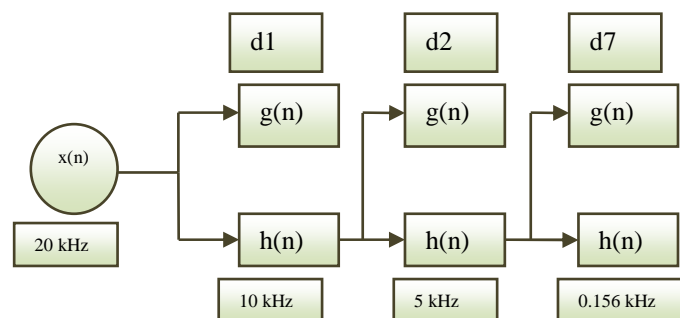


Figure 2. MRA using Wavelet Transform

Table-1 Wavelet level and their corresponding frequency bands for a sampling rate of 20 kHz

Wavelet Level	Frequency Band (Hz)	Center Frequency (Hz)
d1	5000-10000	7500
d2	2500-5000	3750
d3	1250-2500	1875
d4	625-1250	937.5
d5	312.5-625	468.75
d6	156.25-312.5	234.375
d7	78.125-156.25	117.1875

A sampling rate of 20 kHz is selected in this study. Daubechies wavelet db4 is used as the mother wavelet since it has given good performance for power system transient analysis [14], [15]. Based on the sampling rate, the current/voltage signal can be fully decomposed into seven levels as shown in Table I [12], [13]. It is expected that the transient energy will be captured in levels d1–d4 and the energy in level d7 will track the variations of current with frequency around the nominal frequency. WT will decompose the signal into 7 levels d1–d7 as shown in Table I,

each level having detail coefficients. The total energy “D” in each level “d” can be calculated using the Frobenius norm as

$$D = \sqrt{\sum_{i=1}^N [d(i)]^2} \tag{4}$$

The total energy of levels of interest—D7 for the current signal and D1 through D4 for the voltage signal are calculated and tracked. The reason for selecting the voltage signal to track the energy of transients is because faults give rise to more transients in the voltage than in the currents.

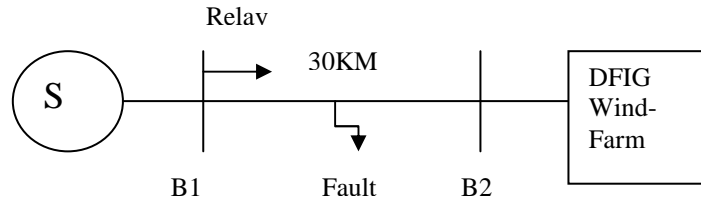


Figure 3. Simulated Systems

Table-2 Parameters of the Transmission line

R1=0.1153 Ω/km	R0=0.413 Ω/km
L1=1.05X10 ⁻³ H/km	L0=3.37X10 ⁻³ H/km
C1=11.33X10 ⁻⁹ F/km	C0=5.01X10 ⁻⁹ F/km

Where

- R1: Positive Sequence Resistance
- R0: Zero Sequence Resistance
- L1: Positive Sequence Inductance
- L0: Zero Sequence Inductance
- C1: Positive Sequence Capacitance
- C0: Zero Sequence Capacitance

3. Simulation Results

Figure 3 shows the system selected for simulation. The system details are given in the Table-2. The system is simulated through MATLAB computer simulation package. The sending end (SE) is modeled as an equivalent machine and the receiving end (RE) is modeled as a DFIG wind-farm. The corresponding results are presented here.

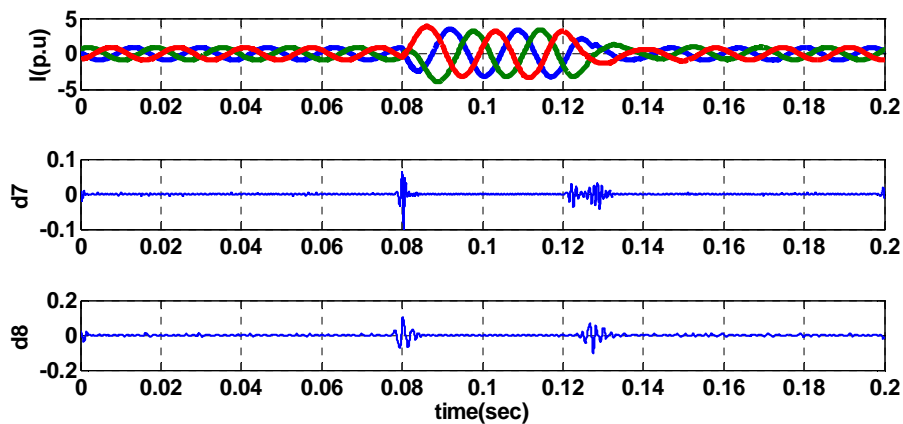


Figure 4. Current, wavelet-d7 and wavelet-d8 results in (LLL-G) faults

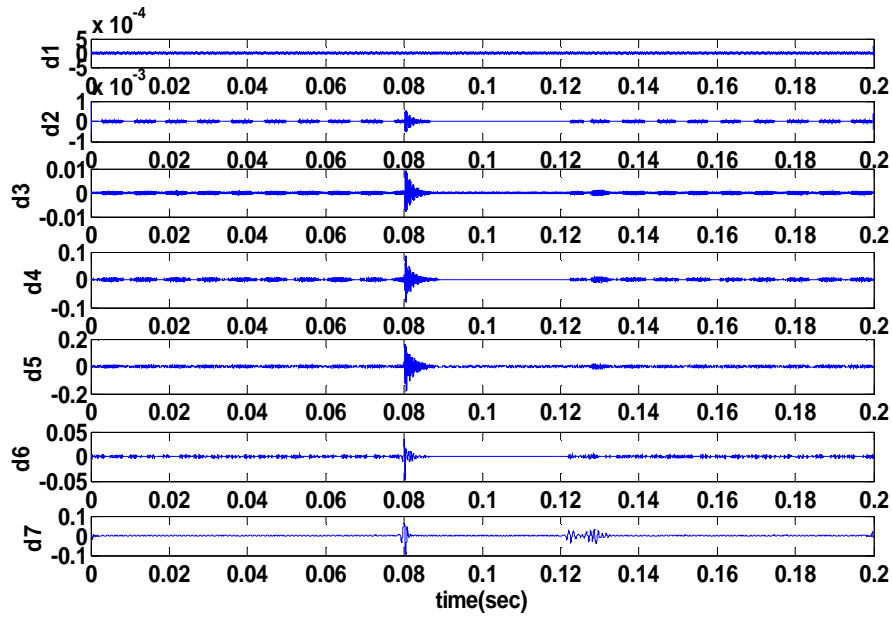


Figure 5. Wavelet- d1 to wavelet-d7 decompose signal

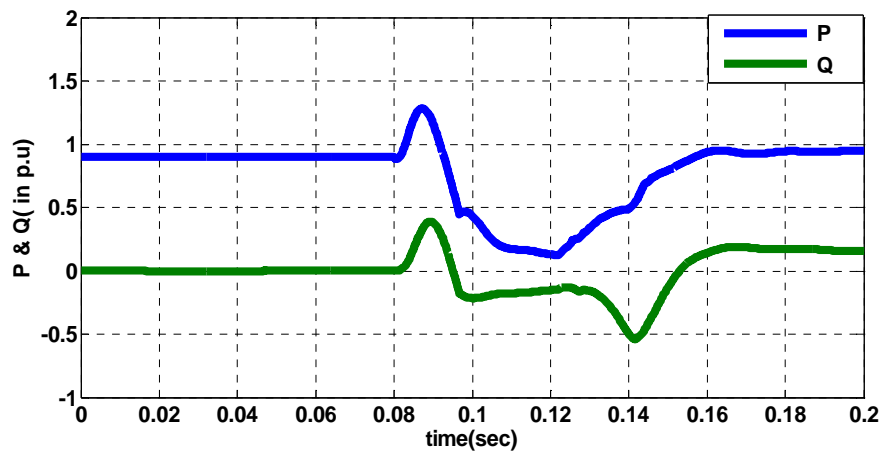


Figure 6. P (active power) and Q (reactive power) during LLL-G faults

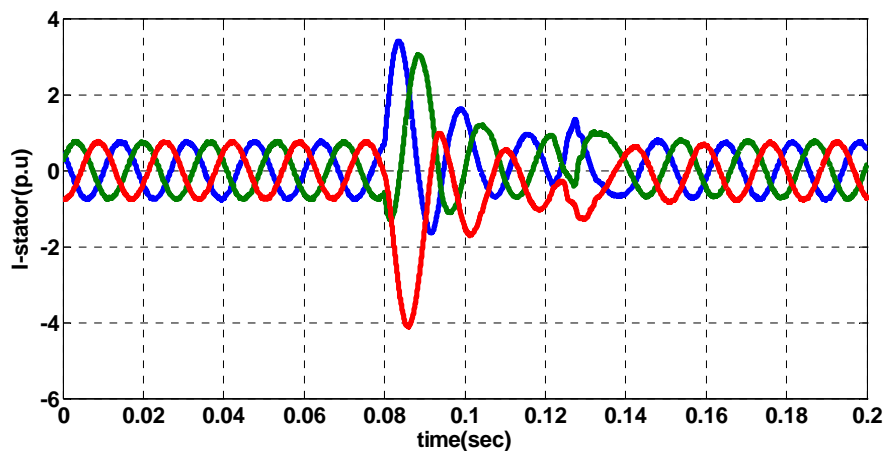


Figure 7. Stator current during LLL-G faults

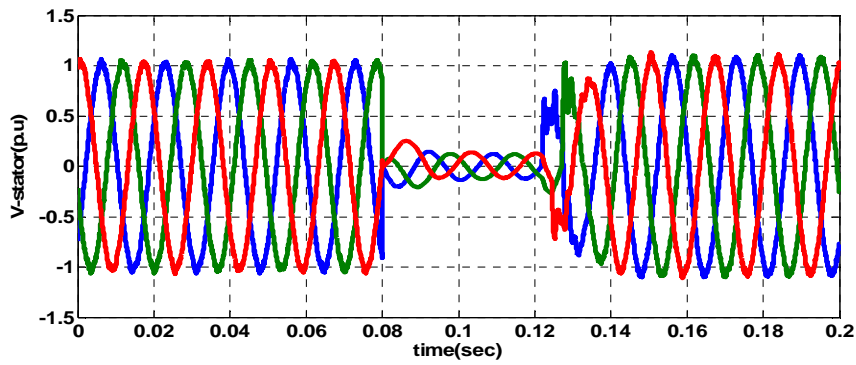


Figure 8. Stator voltage during LLL-G faults

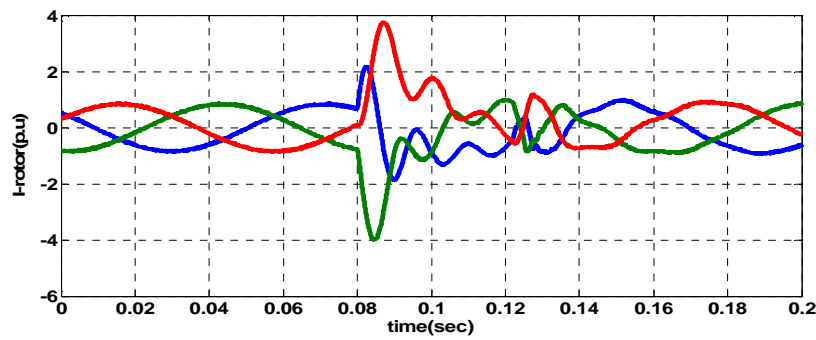


Figure 9. Rotor current signals during LLL-G faults

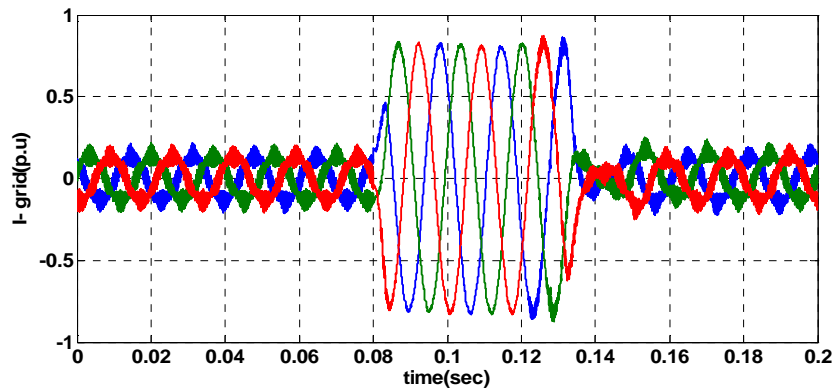


Figure 10. Grid current signals during LLL-G faults

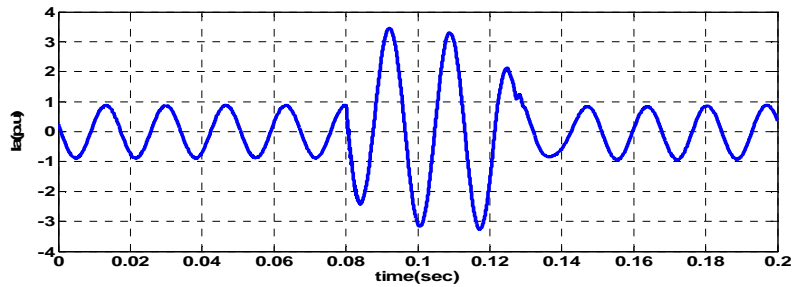


Figure 11. Phase-a current signals at relay end during LLL-G faults

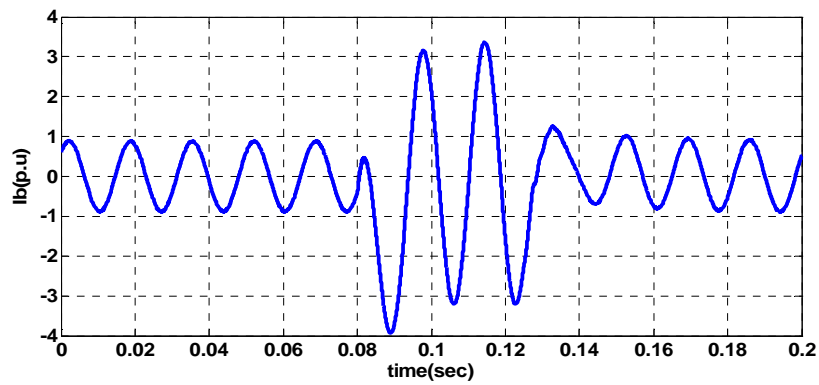


Figure 12. Phase-a current signal at relay end during LLL-G faults

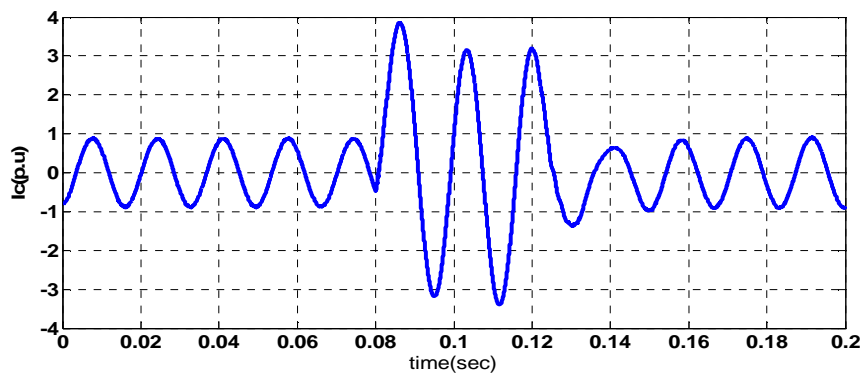


Figure 13. Phase-c current signals at relay end during LLL-G faults

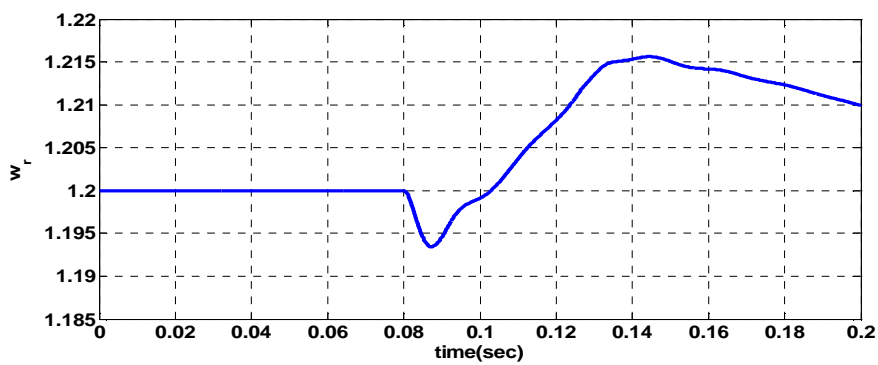


Figure 14. w_r signals during LLL-G faults

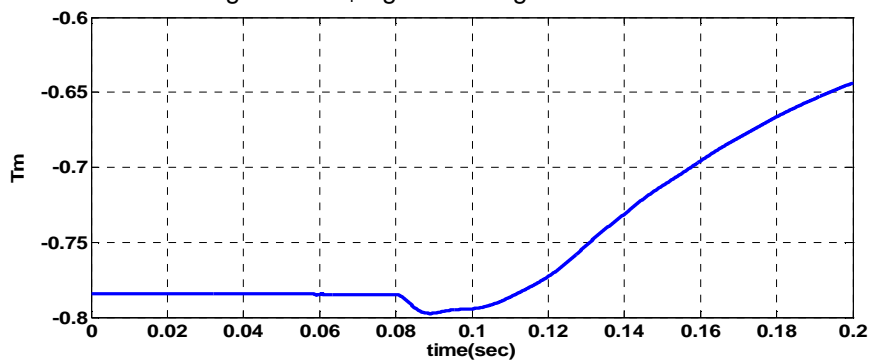


Figure 15. T_m (mech. torque) signals during LLL-G faults

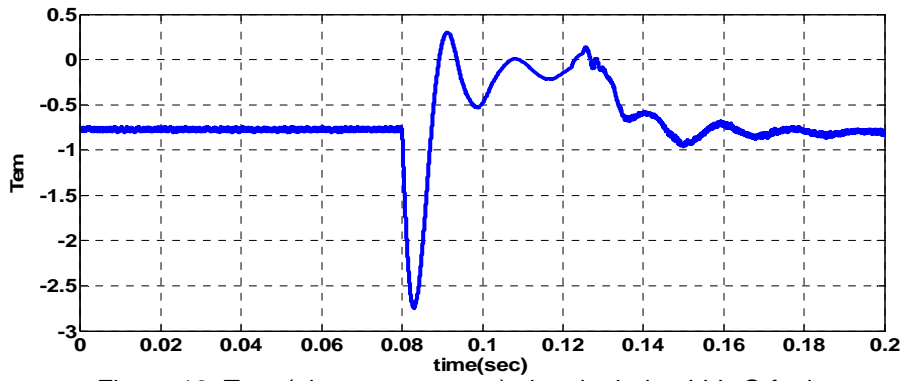


Figure 16. Tem (elec. mag. torque) signals during LLL-G faults

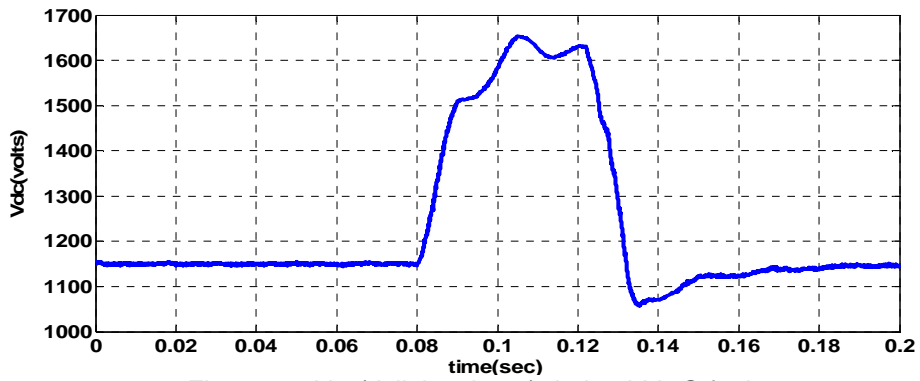


Figure 17. V_{dc} (dclink voltage) during LLL-G faults

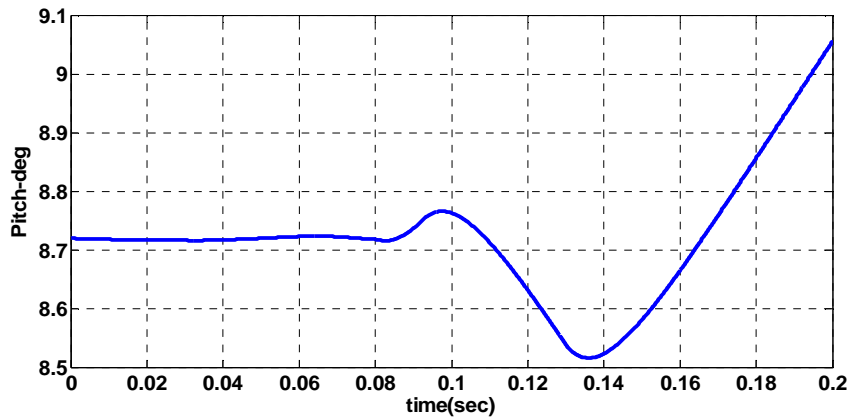


Figure 18. pitch_deg during LLL-G faults

Table –3 Energy of the signals for different wavelet level d1 to d8

Energy of the signals	Without faults	With faults
Ed1	0	0
Ed2	0	0
Ed3	0	0
Ed4	0.0015	0.0009
Ed5	0.0042	0.0046
Ed6	0.0004	0.0003
Ed7	0.0009	0.0024
Ed8	0.0044	0.0086

4. Proposed Wavelet Energy Function for Fault Detection in Presence of DFIG Wind-Farm

The diagram of the proposed asymmetrical fault detection method based on the energy function technique and wavelet transform is conceptually shown in Figure 19.

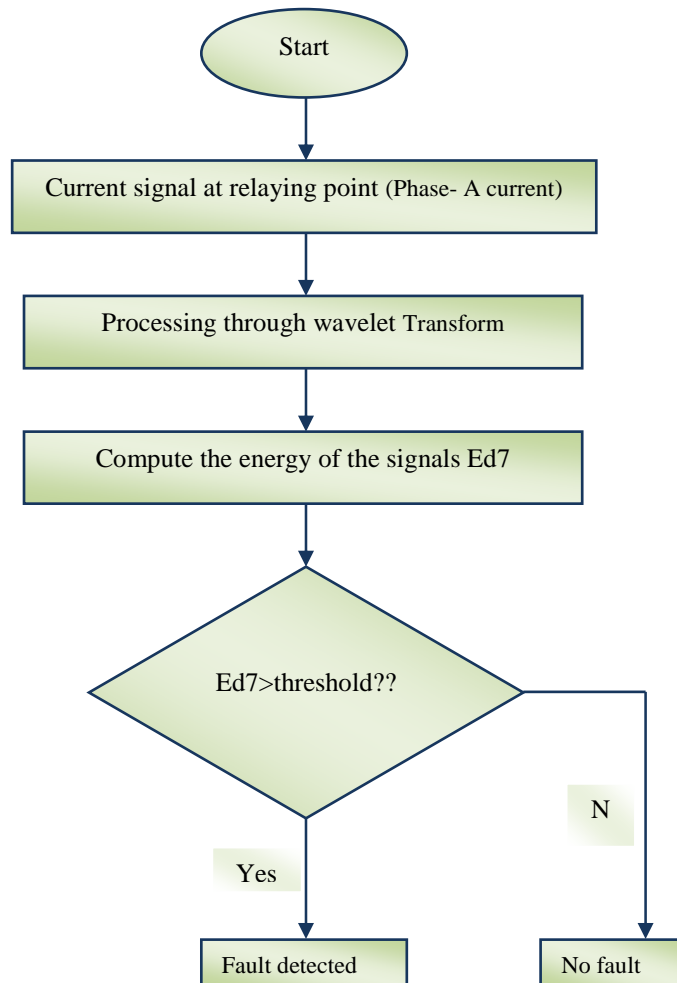


Figure 19. Flow chart for the proposed energy function for fault detection in presence of DFIG wind-farm

4.1 Data Acquisition

The proposed asymmetrical fault detection in presence of DFIG wind-farm requires data acquisition for all three phase currents. Those data can be obtained directly from measurement units of advanced digital relays. Most wavelet transform based methods require high frequency sampling rate. The detection method proposed in this paper can be used in a wide range of sampling rates. Considering advanced digital relays using sampling rate of 10 kHz, the same sampling rate is selected in this study, which can satisfy the requirements of the wavelet transform proposed in this scheme with good results. In order to avoid aliasing due to the fault transients and low sampling rate, an analog antialiasing filter needs to be employed before the sampling of the input waveforms coming from instrument transformers. There are many known solutions available for implementing the antialiasing filters; hence, no further discussion is given.

4.2 Wavelet Transform

The samples are fed to the relay at a reduced rate of 10 kHz, because higher sampling rate is not required for normal relay functions. The samples of the three-phase current of any one phase (say I_A) are processed with WT. Using (1), the indices D1, D2, D3, D4, D5, D6 and D7 are formed for current (I_A).

4.3 Wavelet Energy

After processing through WT. We get indices D1 to D7 and cross ponding that we get Ed1 to Ed7 i.e shown in Table-III clearly.

4.4 Asymmetrical Fault Detection (LLL-G)

After calculating the energy (Ed) for each indices then Comparing Ed7 with E_{th} (without faults) so fault is detected. ($Ed7 > E_{th}$)

5. Conclusion

In this paper, a new technique for detecting asymmetrical fault (LLL-G) in presence of a DFIG has been studied by analyzing the current signal at relay end and the effectiveness of a new and reliable approach for the characterization of asymmetrical fault (LLL-G) in time varying condition is observed. The proposed approach is based on an optimized use of the DWT by a simple pre-processing of the variables to be analyzed. In the case study, the three-phase fault is created in the grid and proposed algorithm detects the fault with in one and half cycles for 60Hz system. A new diagnostic method based on the grid modulating signals pre-processing by Discrete Wavelet Transform (DWT) thereby is proposed here to detect grid faults dynamically over time. From the simulation results, we could observe that, the proposed method not only detects the fault within one and half cycle of fundamental wave, also it reveals the effectiveness under time- varying conditions.

6. References

- [1] L. M. Popa, B. B. Jensen, F. Ritche, and I. Boldea, "Condition monitoring of wind generators," in Conf. Rec. IEEE IAS Annu. Meeting, Oct. 2003, vol. 3, pp. 1839–1846.
- [2] P. Caselitz, J. Giebhardt, T. Kruger, and M. Mevenkamp, "Development of a fault detection system for wind energy converters," in Proc. EUWEC, Göteborg, Sweden, 1996, pp. 1–4.
- [3] Q. F. Lu, C. T. Cao, and E. Ritche, "Model of stator inter-turn short circuit fault in doubly-fed induction generators for wind turbine," in Proc. 35th Annu. IEEE PESC, Jun. 2004, vol. 2, pp. 932–937.
- [4] I. Albizu, A. Tapia, J. R. Saenz, A. J. Mazon, and I. Zamora, "Online stator winding fault diagnosis in induction generators for renewable generation," in Proc. 35th Annu. IEEE PESC, Jun. 2004, vol. 2, pp. 932–937.
- [5] L. H. Hansen, L. Helle, F. Blaabjerg, E. Ritche, S. Munk-Nielsen, H. Bindner, P. Sorensen, and B. Bak-Jensen, "Conceptual survey of generators and power electronics for wind turbines," Risø Nat. Lab., Roskilde, Denmark, Dec. 2001.
- [6] S. Nandi and H. A. Toliyat, "Fault diagnosis of electrical machines A review," in Conf. Rec. 34th IEEE IAS Annu. Meeting, 1999, vol. 1, pp. 197–204.
- [7] P. Vas, Parameter Estimation, Condition Monitoring, and Diagnosis of Electrical Machines. Oxford, U.K.: Clarendon, 1993.
- [8] H. Douglas, P. Pillay, and P. Barendse, "The detection of inter-turn stator faults in doubly-fed induction generators," in Conf. Rec. 40th IEEE IAS Annu. Meeting, Oct. 2–6, 2005, vol. 2, pp. 1097–1102.
- [9] T. Wildi, Electrical Machines, Drives, and Power Systems. 6th ed. Englewood Cliffs, NJ: Prentice-Hall, 2005.
- [10] W. T. Thomson, "On-line MCSA to diagnose shorted turns in low voltage stator windings of 3-phase induction motors prior to failure," in Proc. IEEE-IEMDC, 2001, vol. 1, pp. 891–898.
- [11] J. A. Baroudi, V. R. Dinavahi, and A. M. Knight, "A review of power converter topologies for wind generators," in Proc. IEEE Int. Elect. Mach. Drives, May 15–18, 2005, vol. 1, pp. 458–465.
- [12] C. Parameswariah and M. Cox, "Frequency characteristics of wavelets," IEEE Trans. Power Del., vol. 17, no. 3, pp. 800–804, Jul. 2002.
- [13] D. C. Robertson, O. I. Camps, J. S. Mayer, and W. B. Gish, "Wavelets and electromagnetic power system transient," IEEE Trans. Power Del. vol. 11, no. 2, pp. 1050–1058, Apr. 1996.
- [14] S. Santoso, E. J. Powers, W. M. Grady, and P. Hofmann, "Power quality assessment via wavelet transform analysis," IEEE Trans. Power Del., vol. 11, no. 2, pp. 924–930, Apr. 1996.
- [15] A. Osman and O. P. Malik, "Transmission line distance protection based on wavelet transform," IEEE Trans. Power Del., vol. 19, no. 2, pp. 515–523, Apr. 2004.
- [16] J. Upender, C. P. Gupta and G. K. Singh, "Discrete wavelet transform and probabilistic neural network based algorithm for classification of fault on transmission systems," in India conf. IEEE, INDICON 2008, 11-13 Dec, 2008, Vol. 1, pp. 206-211.